



Manifestations of morphology-dependent resonances in Mie scattering matrices

Michael I. Mishchenko ^{*}, Andrew A. Lacis

NASA Goddard Institute for Space Studies, 2880 Broadway, New York, NY 10025, USA

Abstract

Lorenz–Mie computations of the extinction cross-section for monodisperse spheres show the existence of a very complex structure that includes extremely narrow peaks called morphology-dependent resonances (MDRs). The width and magnitude of the peaks are highly sensitive functions of the size parameter and the refractive index of the sphere. So far the MDRs have been calculated and observed mostly for the total optical cross-sections and the scattered intensity, though it has been clear that they should also exist in the scattering matrix elements. In this paper we use modern visualization techniques to study the manifestations of MDRs in the elements of the Stokes scattering matrix and their dependence on the refractive index. We show that within MDRs, the scattering matrix elements may drastically change not only their magnitude, but also their sign. Even weak absorption inside the particles strongly modifies and then completely destroys the polarization resonance effects. © 2000 Published by Elsevier Science Inc. All rights reserved.

Keywords: Scattering; Electromagnetics; Lorenz–Mie theory; Scattering resonances; Particle characterization

1. Introduction

The light scattering properties of dielectric spheres have been studied extensively since the development of the Lorenz–Mie theory [1]. This theory provides an effective means of quantitative interpretation of measurements of both the intensity and the polarization of scattered light and, thus, the basic

^{*} Corresponding author.

E-mail address: crmim@giss.nasa.gov (M.I. Mishchenko).

foundation of remote sensing and optical particle characterization [2,3]. Yet, there are some relatively recent phenomena of Mie scattering that are less frequently studied and might be considered as perhaps surprising or unexpected behavior [4]. These are the super-narrow resonance spikes called morphology-dependent resonances (MDRs) that were noticed in calculations of the Mie extinction cross-section at high size parameter resolution [5,6]. The theoretical basis for these sharp resonance features and their relative spacing as functions of the particle size parameter and refractive index are well understood as a part of the basic Lorenz–Mie scattering formulation [4–7].

So far the MDRs have been calculated and observed mostly for the total optical cross-sections and the scattered intensity [4–12], though it has been clear that they should also exist in the elements of the Stokes scattering matrix. In this paper we report results of extensive computations and use modern visualization techniques to study the manifestations of MDRs in the scattering matrix elements and their dependence on the real and imaginary parts of the refractive index.

2. Calculations

A detailed overview of the Lorenz–Mie theory can be found in [1]. To ensure high accuracy of calculations, we employed two independently written FORTRAN codes using double-precision floating-point variables and found perfect agreement.

Fig. 1 shows the extinction efficiency factor $Q_{\text{ext}} = C_{\text{ext}}/(\pi a^2)$ and the asymmetry parameter of the phase function g versus size parameter $x = 2\pi a/\lambda$ for monodisperse spherical particles with an index of refraction $m = 1.4$, where C_{ext} is the extinction cross-section, a the radius, and λ is the wavelength. Both curves are characterized by a series of major maxima and minima with superimposed high-frequency ripple and spike-like MDRs. The major maxima and minima are called the “interference structure” since they are traditionally explained as the result of interference of light diffracted and transmitted by the particle [1,2]. A light ray passing through the center of a sphere acquires a phase shift of $\rho = 2x(m_r - 1)$, where m_r is the real part of the refractive index. Therefore, constructive and destructive interference and, thus, maxima and minima in the extinction efficiency curve, occur successively at intervals $\approx 2\pi$ in ρ .

On the other hand, both the ripple and the MDRs are caused by the resonance behavior of the Mie coefficients a_n and b_n [6]. As the size parameter approaches a resonant value, the denominator of a Mie coefficient a_n or b_n approaches a local minimum, thereby causing a local extremum (maximum or minimum) in the curve for a specific scattering characteristic. Interestingly, the numbers of local extrema in the two curves are identical and a local minimum/maximum in the extinction curve always corresponds to a local maximum/minimum in the asymmetry parameter curve.

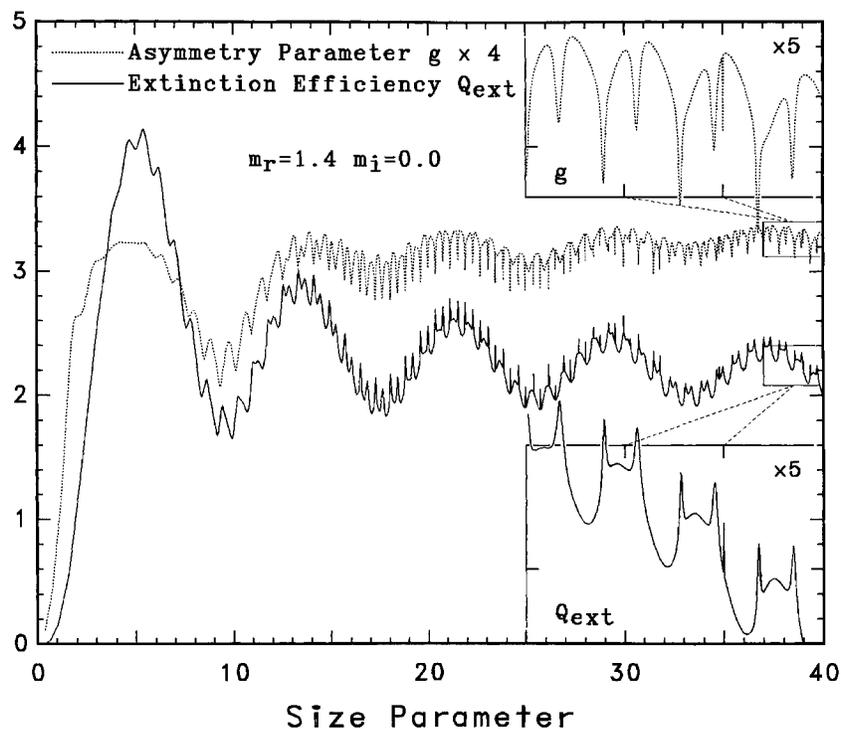


Fig. 1. Extinction efficiency factor Q_{ext} and asymmetry parameter of the phase function g versus size parameter x for monodisperse spherical particles with an index of refraction $m = 1.4$.

The difference between the high-frequency ripple features and the MDRs is that the latter are much narrower. This is demonstrated in Fig. 2 which shows the angular profile of the MDR centered at $x \approx 38.9983$. The dots show the sampling resolution used in Fig. 1, and it was a bare coincidence that the MDR depicted in Fig. 2 also showed up in Fig. 1. This demonstrates once again the extreme narrowness of the MDRs.

Fig. 2 also shows the behavior of the MDR with increasing imaginary part of the refractive index m_i . It is seen that increasing m_i from 0 to a very small value of 10^{-5} almost completely destroys the MDR while not changing whatsoever the background Q_{ext} and g values. Since it takes much larger m_i values in order to eliminate the ripple and the interference structure [13], Fig. 2 suggests that measurements within MDRs may be far more sensitive to weak absorption than measurements in the “continuum”.

It appears that the manifestations of the ripple and the MDRs are even more spectacular in the elements of the Stokes scattering matrix \mathbf{F} than in the integral photometric characteristics. The scattering matrix describes the

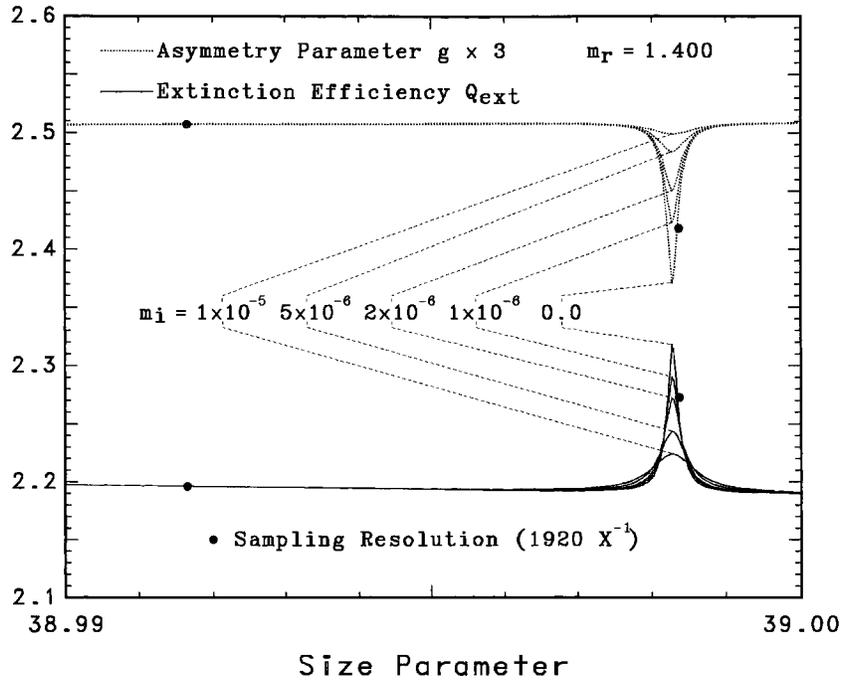


Fig. 2. Profile of the MDR centered at $x \approx 38.9983$ for five values of the imaginary part of the refractive index m_i . The dots show the sampling resolution used in Fig. 1.

transformation of the Stokes vector of the incident light into the Stokes vector of the scattered light:

$$\mathbf{I}^{\text{sca}} \propto \mathbf{F}(\Theta) \mathbf{I}^{\text{inc}}, \quad (1)$$

where Θ is the scattering angle, i.e., the angle between the incident and scattered beams, and

$$\mathbf{I} = \begin{bmatrix} I \\ Q \\ U \\ V \end{bmatrix} \quad (2)$$

is a four-component Stokes vector [1,2]. For spheres, the scattering matrix has the well-known block-diagonal structure [1],

$$\mathbf{F}(\Theta) = \begin{bmatrix} F_{11}(\Theta) & F_{12}(\Theta) & 0 & 0 \\ F_{12}(\Theta) & F_{11}(\Theta) & 0 & 0 \\ 0 & 0 & F_{33}(\Theta) & F_{34}(\Theta) \\ 0 & 0 & -F_{34}(\Theta) & F_{33}(\Theta) \end{bmatrix} \quad (3)$$

and has only four independent elements.

Since the scattering matrix for a fixed refractive index depends on two variables, viz., the size parameter and the scattering angle, it is convenient to visualize the elements of the scattering matrix using two-dimensional color images plotted with fine angular and size parameter sampling resolution [14,15]. Fig. 3 shows the degree of linear polarization $-F_{12}/F_{11}$ (%) as a function of Θ and x for monodisperse spheres with the same refractive index $m = 1.4$. The image was created using the sampling resolution $\Delta\Theta = 1/3^\circ$ and $\Delta x = 0.05$. With the exception of the region of Rayleigh scattering ($x \lesssim 2$), the entire polarization image is a field of sharp, alternating local maxima and minima. The frequencies of the maxima and minima over both Θ and x increase with increasing size parameter. This very complex “butterfly” structure, which appears to be both chaotic and revealing a perceptible order, was first discovered by Hansen and Travis [2] and results from interference effects for particles of a single size. In their paper published 25 years ago, Hansen and Travis could use only the white and black colors and, therefore, blackened the regions of positive polarization and left the regions of negative polarization white. The use of a continuous color bar in Fig. 3 allowed us to build a complete image of the butterfly structure with a detailed gradation of the magnitude of polarization as well as its sign.

Fig. 4 provides a zoomed image of a small part of the field covered by Fig. 3 and reveals with much greater detail the enormous complexity of the interference pattern. Now the sampling resolution ($\Delta\Theta = 0.1^\circ$ and $\Delta x = 0.007$) is fine enough to exhibit several horizontal “dislocations” or “anomalous strips” which are first indicators of MDRs. One of them is centered at $x \approx 38.9983$ and is shown with even greater sampling resolution ($\Delta\Theta = 0.05^\circ$ and $\Delta x = 0.00001$) in Fig. 5. This figure depicts the ratios F_{33}/F_{11} (%) and F_{34}/F_{11} (%) as well as the degree of linear polarization and shows an immense degree of variability within the resonance. Unlike the optical cross-sections (which are positive by definition) and the asymmetry parameter (which may be negative as well as positive), the normalized scattering matrix elements change not only their absolute value by orders of magnitude (rather than by several percent, as Q_{ext} and g) but even their sign. This potentially makes measurements of the normalized scattering matrix elements a much more sensitive detector of MDRs and hence a more powerful particle characterization technique.

Fig. 6 is analogous to Fig. 5, but shows the degree of linear polarization computed for three increasing values of the imaginary part of the refractive index. Although most MDR’s polarization features gradually weaken and ultimately disappear, the narrow minimum, located at $\Theta \approx 76^\circ$ and $x \approx 38.99828$ for $m_i = 0$ (middle panel in Fig. 5), becomes much more pronounced and shifts toward larger Θ and x before it finally disappears at $m_i = 10^{-4}$. This behavior is quite different from that observed for Q_{ext} and g (Fig. 2).

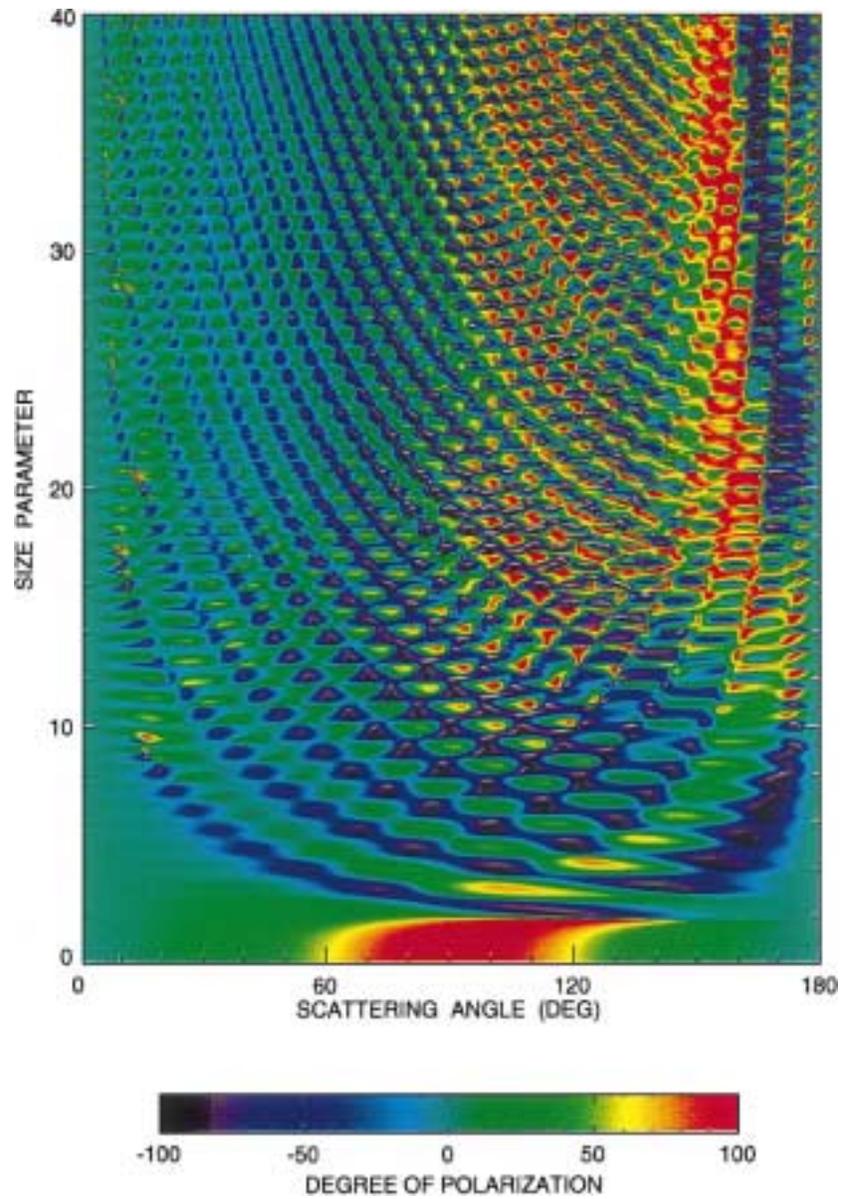


Fig. 3. Low-resolution color image of the degree of linear polarization for monodisperse spherical particles with an index of refraction $m = 1.4$.

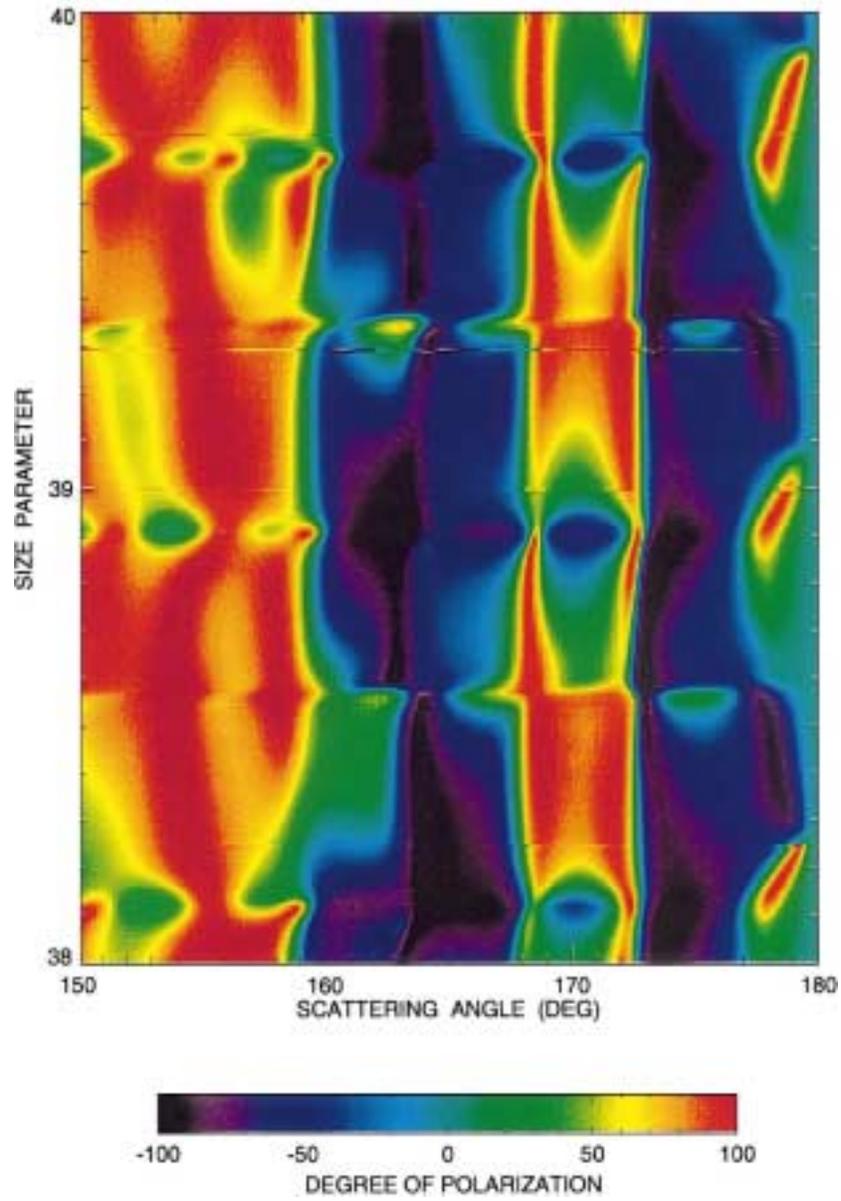


Fig. 4. As in Fig. 3, but using finer sampling resolution.

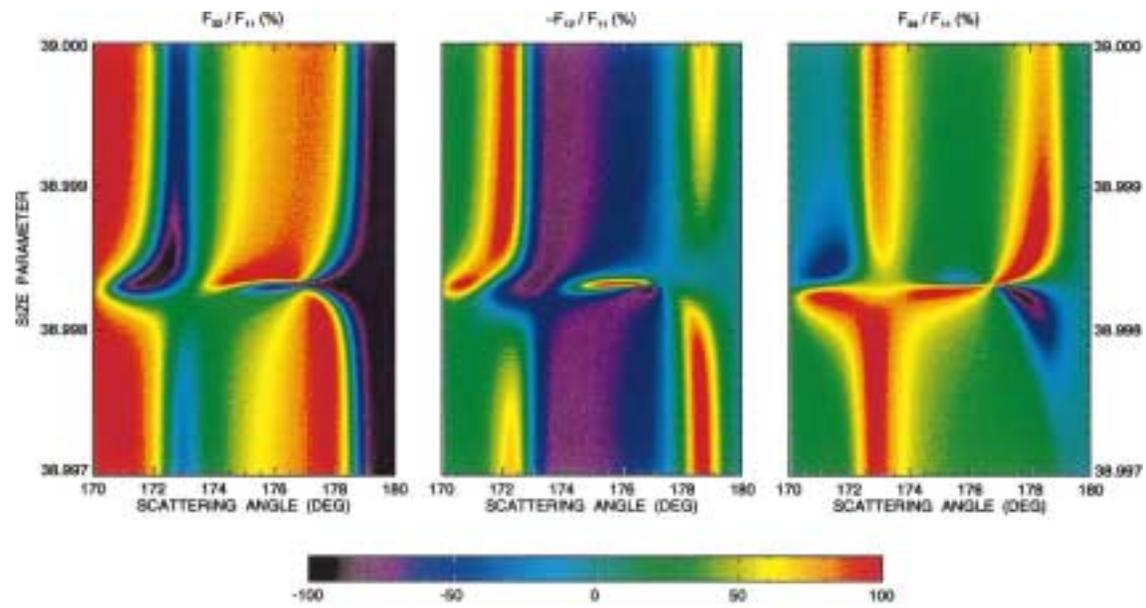


Fig. 5. High-resolution color images of normalized scattering matrix elements within the MDR centered at $x \approx 38.9983$.

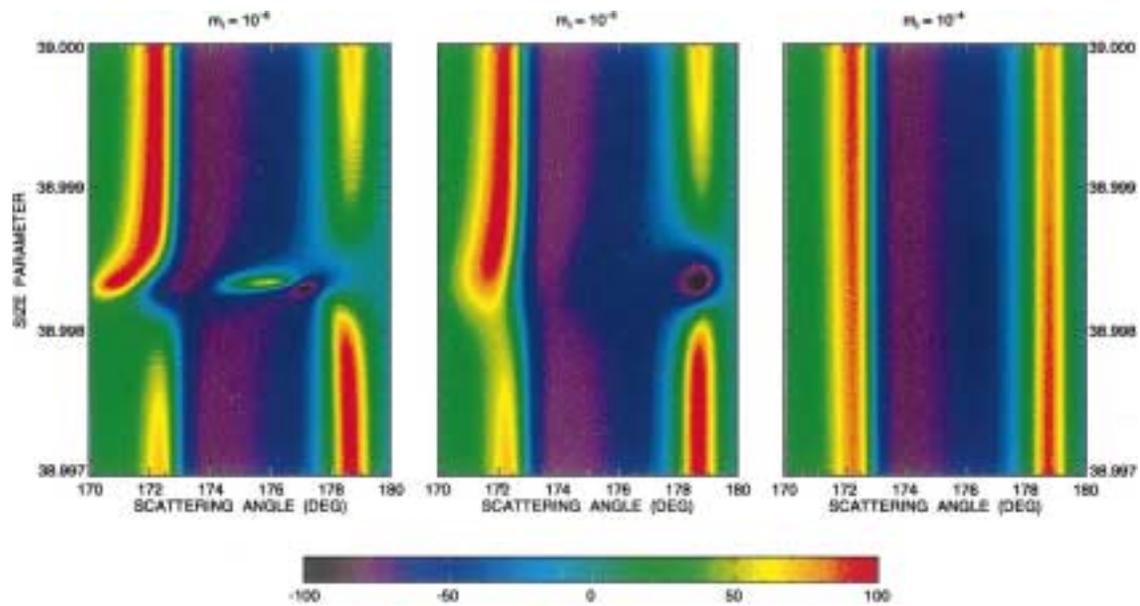


Fig. 6. High-resolution color images of the degree of linear polarization within the MDR centered at $x \approx 38.9983$ for three values of the imaginary part of the refractive index $m_i = 10^{-6}$, 10^{-5} , and 10^{-4} .

Fig. 7 shows the degree of linear polarization versus Θ and m_r for $x = 38.9983$ and $m_i = 0$. Interestingly, this figure is hardly distinguishable from Fig. 5. This strongly suggests that, at least for nonabsorbing particles, the behavior of MDRs is determined by the product of the refractive index and size parameter rather than by each of these quantities separately. This also means that precise measurements of MDRs can be used not only for particle sizing, but also for accurately retrieving the refractive index provided that the particle size is already known.

3. Discussion and conclusions

A natural question to arise is whether the super-sharp MDRs are physically ‘real’, or are artifacts of the theoretical macroscopic concept of ‘sphere’ being applied too literally to microscopic objects. However, high-quality laboratory data, e.g., measurements of the intensity of light scattered by a gradually evaporating $(\text{NH}_4)_2\text{SO}_4$ solution micro-droplet [8], provide an impressive experimental demonstration of the actual occurrence of this phenomenon and its practical usefulness as an optical particle characterization tool [4].

We have demonstrated the spectacular manifestation of MDRs in the normalized elements of the Stokes scattering matrix which includes not only changes in magnitude but also drastic changes in sign within the resonance and a complicated dependence on small values of the imaginary part of the refractive index. It is well known that being intensity ratios, the normalized elements of the scattering matrix, including polarization, can be measured with much higher precision than the scattered intensity itself or the total optical cross-sections [2,16]. Therefore, our results strongly suggest that the potential of using MDRs for optical particle characterization can be significantly enhanced by measuring ratios of the scattering matrix elements. We have also demonstrated that even very weak absorption can strongly modify or completely destroy the polarization pattern of MDRs while leaving the ripple features intact. Therefore, high-precision measurements of MDRs can be used not only for particle sizing or determining the real part of the refractive index, but also for detecting minute deviations of the imaginary part of the refractive index from zero.

The extreme sharpness of the MDR features may also help explain some of the minor, but nevertheless perplexing differences that often show up in inter-comparisons of radiative forcing results and the inter-comparisons of bulk Mie scattering parameters such as the extinction cross-section and asymmetry parameter [17]. In view of the fact that Mie scattering is an exact theory, it follows then that if the particle size and refractive index are agreed upon, precise agreement is expected for the resultant Mie parameters to many decimal places. Thus, the first step in model inter-comparisons should be to verify that the Mie

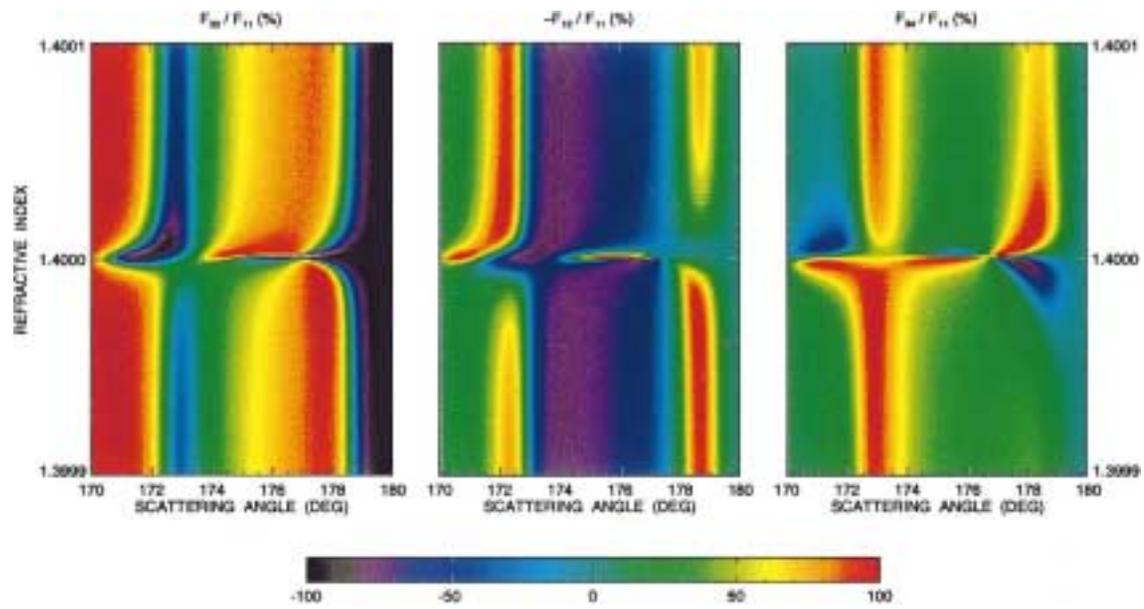


Fig. 7. High-resolution color images of normalized scattering matrix elements versus θ and m_r for $x = 38.9983$ and $m_i = 0$.

codes produce identical results for the same monodisperse size parameter and refractive index. Since the bulk extinction cross-section and asymmetry parameter imply integration over a size distribution of particles, it is clear from the results in Figs. 1 and 2 that convergence is not going to be uniformly monotonic as the number of integration points is increased. Thus, when an integration mesh point hits an MDR feature, there may be an apparent local discontinuity that is greater than 5% compared to the background value. For precise Mie scattering characteristics, exceedingly high resolution in size parameter space is needed to fully resolve the MDR features.

Acknowledgements

This research was sponsored by the NASA Radiation Science Program managed by Robert Curran and the DOE ARM Program. We thank Nadia Zakharova for help with graphics.

References

- [1] H.C. van de Hulst, *Light Scattering by Small Particles*, Wiley, New York, 1957.
- [2] J.E. Hansen, L.D. Travis, Light scattering in planetary atmospheres, *Space Sci. Rev.* 16 (1974) 527–610.
- [3] G. Gouesbet, G. Gréhan, *Optical Particle Sizing: Theory and Practice*, Plenum Press, New York, 1988.
- [4] S.C. Hill, R.E. Benner, Morphology-dependent resonances, in: P.W. Barber, R.K. Chang (Eds.), *Optical Effects Associated with Small Particles*, World Scientific, Singapore, 1988, pp. 3–61.
- [5] P. Chýlek, J.T. Kiehl, M.K.W. Ko, Narrow resonance structure in the Mie scattering characteristics, *Appl. Opt.* 17 (1978) 3019–3021.
- [6] P.R. Conwell, P.W. Barber, C.K. Rushforth, Resonant spectra of dielectric spheres, *J. Opt. Soc. Amer. A* 1 (1984) 62–67.
- [7] G. Videen, J. Li, P. Chýlek, Resonances and poles of weakly absorbing spheres, *J. Opt. Soc. Amer. A* 12 (1995) 916–921.
- [8] P. Chýlek, Resonance structure of Mie scattering: distance between resonances, *J. Opt. Soc. Amer. A* 7 (1990) 1609–1613.
- [9] I.N. Tang, H.R. Munkelwitz, Simultaneous determination of refractive index and density of an evaporating aqueous solution droplet, *Aerosol Sci. Technol.* 15 (1991) 201–207.
- [10] P. Chýlek, D. Ngo, R.G. Pinnick, Resonance structure of composite and slightly absorbing spheres, *J. Opt. Soc. Amer. A* 9 (1992) 775–780.
- [11] D. Ngo, R.G. Pinnick, Suppression of scattering resonances in inhomogeneous microdroplets, *J. Opt. Soc. Amer. A* 11 (1994) 1352–1359.
- [12] F. Borghese, P. Denti, R. Saija, M.A. Iatì, O.I. Sindoni, Optical resonances of spheres containing an eccentric spherical inclusion, *J. Opt.* 29 (1998) 28–34.
- [13] C.F. Bohren, D.R. Huffman, *Absorption and Scattering of Light by Small Particles*, Wiley, New York, 1983, p. 307.
- [14] M.I. Mishchenko, L.D. Travis, Light scattering by polydisperse rotationally symmetric nonspherical particles: linear polarization, *J. Quant. Spectrosc. Radiat. Transfer* 51 (1994) 759–778.

- [15] M.I. Mishchenko, D.W. Mackowski, L.D. Travis, Scattering of light by bispheres with touching and separated components, *Appl. Opt.* 34 (1995) 4589–4599.
- [16] J.W. Hovenier, Measuring scattering matrices of small particles at optical wavelengths, in: M.I. Mishchenko, J.W. Hovenier, L.D. Travis (Eds.), *Light Scattering by Nonspherical Particles: Theory, Measurements, and Applications*, Academic Press, San Diego, 1999, pp. 355–365.
- [17] O. Boucher, S.E. Schwartz, T.P. Ackerman, T.L. Anderson, B. Bergstrom, B. Bonnel, P. Chýlek, A. Dahlback, Y. Fouquart, Q. Fu, R.N. Halthore, J.M. Haywood, T. Iversen, S. Kato, S. Kinne, A. Kirkevag, K.R. Knapp, A. Lacis, I. Laszlo, M.I. Mishchenko, S. Nemesure, V. Ramaswamy, D.L. Roberts, P. Russell, M.E. Schlesinger, G.L. Stephens, R. Wagener, M. Wang, J. Wong, F. Yang, Intercomparison of models representing direct shortwave radiative forcing by sulfate aerosols, *J. Geophys. Res.* 103 (1998) 16979–16998.